THE ASTROPHYSICAL JOURNAL, 498:497–503, 1998 May 10

SMALL-SCALE PERTURBATIONS IN A GENERAL MIXED DARK MATTER COSMOLOGY

WAYNE HU[1] AND DANIEL J. EISENSTEIN
Institute for Advanced Study, Princeton, NJ 08540
Received 1997 September 19; accepted 1997 December 23

ABSTRACT

For a universe with massive neutrinos, cold dark matter, and baryons, we solve the linear perturbation equations *analytically* in the small-scale limit and find agreement with numerical codes at the 1%–2% level. The inclusion of baryons, a cosmological constant, or spatial curvature reduces the small-scale power and tightens limits on the neutrino density from observations of high-redshift objects. Using the asymptotic solution, we investigate neutrino infall into potential wells and show that it can be described on *all* scales by a growth function that depends on time, wavenumber, and cosmological parameters. The growth function may be used to scale the present-day transfer functions back in redshift. This allows us to construct the time-dependent transfer function for each species from a single master function that is independent of time, cosmological constant, and curvature.

Subject headings: cosmology: theory — dark matter — large-scale structure of universe

1. INTRODUCTION

The mixed dark matter (MDM) scenario for structure formation involves a hot component of massive neutrinos as well as the usual cold and baryonic dark matter components. In this case, even calculations in linear perturbation theory are nontrivial due to the time-dependent energy-momentum relation and nonvanishing angular moments of the neutrino distribution. Perturbations no longer grow uniformly with time independent of scale. Specifically, the growth of fluctuations is suppressed below the time-dependent free-streaming scale of the neutrinos due to collisionless damping. Numerical calculations with state-of-the-art Boltzmann codes (e.g., Ma & Bertschinger 1995; Dodelson, Gates, & Stebbins 1996; Seljak & Zaldarriaga 1996) still require a fair amount of time to solve the evolution equations on small spatial scales. Moreover, the additional parameter represented by the neutrino mass m_ν makes an exhaustive search of parameter space more difficult and has led most workers to date to fix parameters such as the baryon density (see, e.g., Ma 1996). For these reasons, we consider here an analytic treatment of small-scale perturbation theory in MDM cosmologies.

The inclusion of baryonic dark matter further complicates the dynamics. Recent measurements of high-redshift deuterium abundances (Tytler et al. 1996; but see Rugers & Hogan 1996) and new theoretical interpretations of the Lyα forest (Weinberg et al. 1997 and references therein) suggest a value of the baryon density Ω_b greater than the fiducial nucleosynthesis value of $0.0125\ h^{-2}$ (Walker et al. 1991). Baryons suppress fluctuations on small scales because, prior to recombination, photon pressure from the cosmic microwave background (CMB) supports them against collapse. Hu & Sugiyama (1996, hereafter HS96) developed a formalism to account for this effect and to solve the evolution equations exactly on small scales. The key aspect to the treatment is the ability to ignore completely the role of baryons as a gravitational source for enhancing cold dark matter (CDM) fluctuations.

Massive neutrinos act in a manner similar to the prerecombination baryons. On scales smaller than their free-streaming length, the neutrinos are smoothly distributed and hence do not contribute to the growth of perturbations. Here we generalize the techniques of HS96 to include the hot component, thereby allowing us to solve analytically for the transfer function on the smallest scales. We then consider how to describe the end of free streaming and the resulting infall of neutrinos into the existing potential wells. This allows us to collapse all of the late-time neutrino effects and to base the transfer function on a single time-independent function of scale.

In an MDM cosmology with realistic baryon content, the amplitude of small-scale fluctuations is important due to growing evidence of early structure formation from high-redshift observations. The model has difficulty in explaining observations of galaxies at redshift $z \sim 3$ (Steidel et al. 1996; Mo & Fukugita 1996) as well as damped Lyα systems at a comparable redshift (Mo & Miralda-Escudé 1994; Kauffmann & Charlot 1994; Klypin et al. 1995; Ma et al. 1997). Baryons only exacerbate this problem and tighten the upper limit on Ω_ν. Indeed, they yield a stronger effect for MDM as compared to CDM cosmologies because $\Omega_b/(\Omega_0 - \Omega_\nu)$ rather than Ω_b/Ω_0 enters into the fluctuation amplitude. Similarly, the growth rate of fluctuations is determined by Ω_ν/Ω_0, such that a given Ω_ν causes more suppression in a low-density universe. Our results here should therefore aid in the investigation of the parameter space left available to MDM cosmologies.

The outline of this paper is as follows. After establishing the notation in § 2, we present in § 3 the small-scale solutions of the perturbation equations derived in the Appendix. We use these solutions in § 4 to study the behavior of neutrino infall and to find analytic approximations thereof. From these results, we construct in § 5 the transfer functions in time and wavenumber for the CDM and total density perturbations and find agreement at the percent level with analytic results in the small-scale limit. In § 6 we show how these results may be scaled to cosmologies with a cosmological constant or spatial curvature.

2. NOTATION

We begin by establishing the notation used throughout. The density of the ith particle species ($i = c$, CDM; b, baryonic dark matter; ν, massive neutrinos) today in units of the critical density is denoted Ω_i, whereas the fraction of the

[1] Alfred P. Sloan Fellow.

total matter density today, $\Omega_0 = \sum_i \Omega_i$, is denoted $f_i = \Omega_i/\Omega_0$. As shorthand, we employ, for example, $i = cb$ to denote $f_{cb} = f_c + f_b$. Note that $f_c + f_b + f_\nu = 1$. Density perturbations are expressed as $\delta\rho_i/\rho_i = \delta_i$, where the hybrid combinations are density weighted (e.g., $\delta_{cb} = f_c\,\delta_c + f_b\,\delta_b$). The CMB temperature is given by $T_{\rm CMB} = 2.7\Theta_{2.7}$ K; the best determination to date is 2.728 ± 0.004 K (Fixsen et al.1996; 95% confidence interval), at which it is fixed for most of our expressions. Finally, as usual the Hubble constant is written as $H_0 = 100\,h\,{\rm km\,s^{-1}\,Mpc^{-1}}$.

Time is parameterized as $y = (1 + z_{\rm eq})/(1 + z)$, where

$$z_{\rm eq} = 2.50 \times 10^4 \Omega_0 h^2 \Theta_{2.7}^{-4} \tag{1}$$

is the redshift of matter-radiation equality. The second important epoch is when the baryons are released from the Compton drag of the photons near recombination, i.e., $y_d = y(z_d)$, where (HS96; Eisenstein & Hu 1998a)

$$\begin{aligned} z_d &= 1291\,\frac{(\Omega_0 h^2)^{0.251}}{1 + 0.659(\Omega_0 h^2)^{0.828}}\,[1 + b_1(\Omega_b h^2)^{b_2}]\,, \\ b_1 &= 0.313(\Omega_0 h^2)^{-0.419}[1 + 0.607(\Omega_0 h^2)^{0.674}]\,, \\ b_2 &= 0.238(\Omega_0 h^2)^{0.223}\,. \end{aligned} \tag{2}$$

After this epoch, baryons fall into the potential wells provided by the CDM and participate in gravitational collapse.

We often label the comoving wavenumber k relative to the scale that crosses the horizon at matter-radiation equality, thus defining the quantity

$$\begin{aligned} q &= \frac{k}{\rm Mpc^{-1}}\,\Theta_{2.7}^2(\Omega_0 h^2)^{-1} \\ &= \frac{k}{19.0}\,(\Omega_0 H_0^2)^{-1/2}(1 + z_{\rm eq})^{-1/2}\,. \end{aligned} \tag{3}$$

The small-scale limit is defined as $q \gg 1$. In the next section (§ 3), we place an additional restriction that the momentum of the neutrinos keep them out of the perturbations formed by the heavier species. Such scales are below the *free-streaming* scale, which itself shrinks with time (cf. eq. [12]). We show in § 4 how to account for neutrino infall.

We often encounter functions of wavenumber or time that depend additionally on cosmological parameters; we denote these as, e.g., $F(y, q; f_\nu \ldots)$. Where the cosmological parameter dependence is not being emphasized, we often drop the parameters after the semicolon, e.g., $F(y, q) \equiv F(y, q; f_\nu \ldots)$.

3. SMALL-SCALE SOLUTION

Below the free-streaming scale of the neutrinos (see § 4) and sound horizon of the baryons at recombination, the equations of motion for matter density fluctuations may be solved analytically in a matter plus radiation universe using the techniques of HS96. The key approximation is that on sufficiently small scales the neutrinos move too quickly to trace the perturbations in the CDM and baryons. In this case the neutrinos contribute no gravitational sources to the evolution equations of the other species, thereby slowing the growth of fluctuations. The baryons have a similar behavior prior to the drag epoch; in the Appendix we describe how to include both effects.

The result is that density perturbations grow as

$$\delta_{cb}(y, q; f_\nu, f_b, y_d) = D_{cb}(y; f_\nu)\delta_d(q; f_\nu, f_b, y_d)\,. \tag{4}$$

Equation (4) states that the density perturbation today is the product of a growth function D_{cb} that depends on the neutrino fraction and the amplitude δ_d of fluctuations entering the growing mode at the Compton drag epoch y_d.

The quantity

$$p_i(f_i) = \tfrac{1}{4}(5 - \sqrt{1 + 24 f_i}) \geq 0 \tag{5}$$

determines the reduction from a linear growth rate $\delta \propto y$, where f_i is the fractional density in gravitationally clustering components: $i = c$ and $i = cb$ before and after the drag epoch, respectively. Hence, the growth factor is given by (Bond et al. 1980)

$$D_{cb}(y; f_\nu) = y^{1 - p_{cb}}\,, \tag{6}$$

where we take $\Omega_0 = 1$; we generalize to $\Omega_0 \neq 1$ in § 6.

The amplitude of the fluctuation entering the growing mode at the drag epoch is (cf. eq. [A6])

$$\delta_d(q; f_\nu, f_b, y_d) = 9.50 M_d(q)\Phi(0, q)\,, \tag{7}$$

where $\Phi(0, q)$ is the initial amplitude of the potential perturbation deep in the radiation-dominated epoch. The quantity M_d expresses the matching condition between the growing mode y^{1-p_c} before the drag epoch and $y^{1-p_{cb}}$ after the drag epoch, as well as the matching required to describe the onset of matter domination. We find

$$\begin{aligned} M_d(q; f_\nu, f_b, y_d) = \frac{f_c}{f_{cb}}\,\frac{5 - 2(p_c + p_{cb})}{5 - 4p_{cb}}\,(1 + y_d)^{p_{cb} - p_c} \\ \times \left\{1 + \frac{p_c - p_{cb}}{2}\left[1 + \frac{1}{(3 - 4p_c)(7 - 4p_{cb})}\right]\right. \\ \left. \times\,(1 + y_d)^{-1}\right\} A_1(q)\,, \end{aligned} \tag{8}$$

where[2]

$$A_1(q; f_{\nu b}, f_\nu) = \frac{1 - 0.553 f_{\nu b} + 0.126 f_{\nu b}^3}{1 - 0.193 f_\nu^{1/2} + 0.169 f_\nu}\,\ln(1.84\beta_c\, q)\,, \tag{9}$$

$$\beta_c = (1 - 0.949 f_{\nu b})^{-1}\,. \tag{10}$$

Equation (8) results from a series expansion in $(1 + y_d)^{-1}$ of the analytic solution and accounts for small deviations from the power-law growing-mode behavior due to radiation. The expansion is only accurate for $f_b + f_\nu \lesssim 0.6$ and $y_d \gtrsim 1$, but the form in the Appendix is general. Notice that $M_d \to A_1$ as $f_b \to 0$ and that the term in brackets in equation (8) introduces only a small correction since $y_d \gtrsim 1$ in cases of interest.

In Figure 1 we display an example of the time evolution of a mode given by the analytic solution (including here the decaying mode given in the Appendix, important for $y \lesssim y_d$) compared with numerical solutions. The 5% offset at early times is due to changes in the expansion rate as the neutrinos become nonrelativistic. The oscillatory errors arise from neglect of baryon acoustic oscillations; these damp away well before the drag epoch for these scales. The main effect of the neutrinos is to slow the growth of the CDM and baryons after equality ($y > 1$) because they represent a smooth gravitationally stable component on these scales. Similarly, since the baryons have no fluctuations on these scales until they fall into CDM potential wells after the drag epoch y_d, they reduce the growth rate between equality and

[2] We assume here the number of massive neutrinos $N_\nu = 1$; see eq. (A17) for the general case.

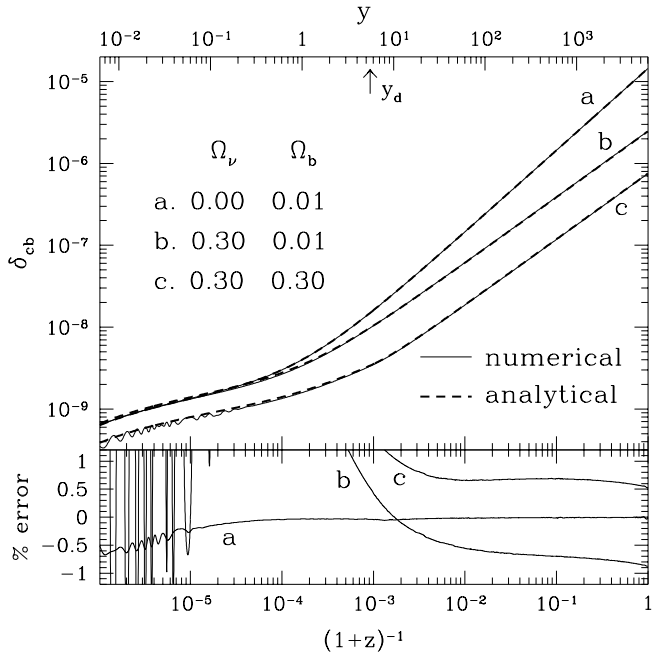

FIG. 1.—Growth suppression from the neutrinos and baryons. The addition of neutrinos slows the growth of CDM plus baryon fluctuations after matter-radiation equality $y > 1$ (*upper panel, curve a compared with curve b*). Increasing the baryon fraction further suppresses fluctuations by a time-independent factor at $y > y_d$ due to growth suppression in the CDM fluctuations for $1 < y < y_d$ and the lack of baryon fluctuations in the weighted density perturbations (*upper panel, curve c*). The analytic expressions (*dashed lines*) agree with numerical results (*solid lines*) for $\Omega_0 = 1$ and $h = 0.5$ at the 1% level except for 5% discrepancies at $y \leq 1$ (*lower panel*). The scale here is $q = 160$ and is chosen to be well in the free-streaming regime.

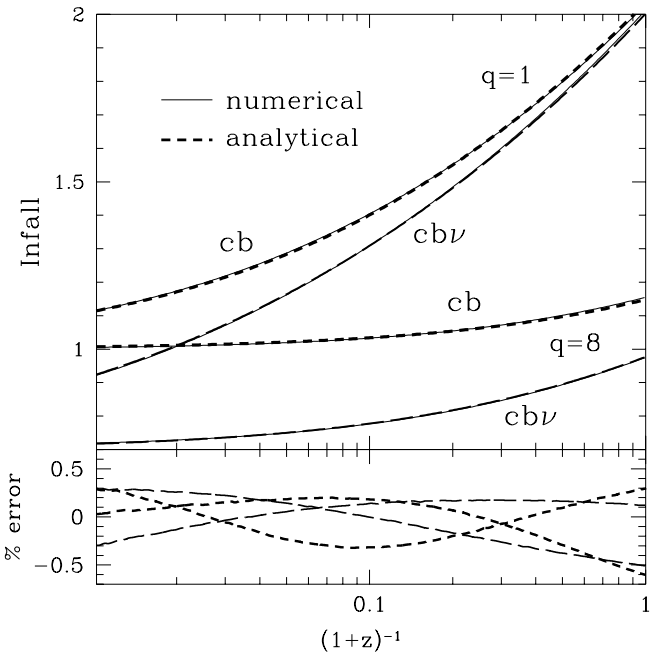

FIG. 2.—Analytic vs. numerical descriptions of neutrino infall for $f_\nu = 0.3, f_b = 0.01, \Omega_0 = 1, h = 0.5$. *Upper panel*: Growth functions compared to the fully free-streaming time dependence of $y^{1-p_{cb}}$; the case without infall is represented by a horizontal line of amplitude 1 (*cb*) and $f_{cb} = 0.69$ (*cbν*) here. Numerical CDM plus baryon fluctuations are compared with growth function D_{cb} (*short-dashed lines*) and numerical CDM plus baryon plus neutrino density-weighted fluctuations with $D_{cb\nu}$ (*long-dashed lines*). *Lower panel*: Relative error.

the drag epoch. Furthermore, they reduce the net fluctuation δ_{cb} as f_c/f_{cb} leads to the offset between the curves b and c in Figure 1 (*upper panel*).

4. NEUTRINO INFALL

Eventually, the neutrinos fall into the CDM potential wells, breaking the approximation of the last section. The neutrino thermal velocity decays with the expansion of the universe as $v_\nu \propto (am_\nu)^{-1}$; infall occurs when their velocity slows sufficiently to allow clustering by the Jeans criteria (Bond & Szalay 1983; Ma 1996):

$$k_{\rm fs} = (4\pi G\rho a^2/v_\nu^2)^{1/2} \propto (1+z)^{-1/2}(\Omega_0 h^2)^{3/2}(f_\nu/N_\nu)\,,$$
$$q_{\rm fs} \propto y^{1/2}(f_\nu/N_\nu)\,, \qquad (11)$$

where the subscript "fs" denotes free streaming. Recall that k and q are related by equation (3). Here N_ν is the number of massive neutrino species, assumed to be degenerate in mass. For simplicity, we restrict our examples to $N_\nu = 1$ throughout, but we have verified that the infall description is valid for $N_\nu \neq 1$ at the 1%–2% level in the range $0 \leq z \leq 25$.[3]

On scales $q \ll q_{\rm fs}$, the neutrinos will follow the CDM. By acquiring density perturbations, they enhance the CDM plus baryon potential wells and drive the growth rate back up to y. Figure 2 (*cb curves*) shows the growth rate of two modes relative to that in the free-streaming regime $y^{1-p_{cb}}$. Because small-scale perturbations begin in the free-streaming regime, these curves go to unity asymptotically at early times. At some epoch $y_{\rm fs}(q)$, which increases with q, the free-streaming scale drops below the wavelength of the perturbation, causing a relative enhancement that scales as $(y/y_{\rm fs})^{p_{cb}}$.

The transition epoch $y_{\rm fs}$ actually incorporates two effects. The first is that from equation (11), the characteristic epoch for infall for a given wavenumber must scale as $y \propto (qN_\nu/f_\nu)^2$. The second is that the growing modes of the free-streaming epoch $\propto y^{1-p_{cb}}$ and the infall epoch $\propto y$ must be matched across the transition. This matching condition may only depend on f_ν. We find that the total effect is well approximated by

$$y_{\rm fs}(q; f_\nu) = 17.2 f_\nu (1 + 0.488 f_\nu^{-7/6})(qN_\nu/f_\nu)^2\,, \qquad (12)$$

The growth rate of the CDM plus baryon density fluctuations can be described by smoothly interpolating the analytic results across $y_{\rm fs}$:

$$D_{cb}(y, q; f_\nu) = \left\{1 + \left[\frac{y}{1 + y_{\rm fs}(q; f_\nu)}\right]^{0.7}\right\}^{p_{cb}/0.7} y^{1-p_{cb}}\,, \qquad (13)$$

where the coefficient 0.7 represents a fit to the numerical evolution. In Figure 2 we compare this expression to numerical solutions (*short-dashed lines*) and find excellent agreement.

Furthermore, the density-weighted fluctuation

$$\delta_{cb\nu} = f_{cb}\,\delta_{cb} + f_\nu\,\delta_\nu \qquad (14)$$

[3] Effects at redshifts approaching the epoch at which the neutrinos become nonrelativistic are not accounted for by this approximation. For $N_\nu \neq 1$, the growth function of eq. (13) allows scaling at low redshifts, but this does not imply that δ_d or $T_{\rm master}$ is independent of N_ν around the maximal infall scale. We treat these effects in Eisenstein & Hu (1998b).

follows from the infall solution by noting that it converges above the free-streaming scale to δ_{cb} and below to $f_{cb}\,\delta_{cb}$. Thus

$$\delta_{cbv}(y, q; f_\nu, f_b, y_d) = D_{cbv}(y, q; f_\nu)\delta_d(q; f_\nu, f_b, y_d)\,, \quad (15)$$

where

$$D_{cbv}(y, q; f_\nu) = \left\{ f_{cb}^{0.7/p_{cb}} + \left[\frac{y}{1 + y_{\rm fs}(q; f_\nu)} \right]^{0.7} \right\}^{p_{cb}/0.7} y^{1-p_{cb}}\,. \quad (16)$$

In Figure 2 (*cbv curves*) we show that this form produces a good fit to the numerical results (*lower set, long-dashed lines*). Note that no infall here is represented by a horizontal line at $f_{cb} = 0.69$.

Finally, the horizon at the epoch when the neutrinos become nonrelativistic sets the maximal free-streaming scale. Beyond this scale, the neutrinos are always in the infall regime, and the evolution of density fluctuations becomes independent of the neutrino fraction:

$$\lim_{q\to 0} \delta_{cb}(y, q) = \frac{1}{137q^2}\, y\Phi(0, q)\,. \quad (17)$$

The appearance of $y/(1 + y_{\rm fs})$ in equation (13) ensures the proper time dependence for the evolution in the large-scale limit. The growth functions are thus not subject to a small-scale approximation and remain valid for all q.

5. TRANSFER FUNCTIONS

We are now in a position to evaluate the transfer function defined as

$$T_i(y, q) = \frac{\delta_i(y, q)}{\delta_i(y, 0)} \frac{\Phi(0, 0)}{\Phi(0, q)} \quad (18)$$

for the ith component of the matter. For the CDM plus baryon ($i = cb$) and the CDM plus baryon plus neutrino ($i = cbv$) systems, we obtain

$$T_{cb}(y, q; f_\nu, f_b, y_d) = y^{-1} D_{cb}(y, q; f_\nu) T_{\rm master}(q; f_\nu, f_b, y_d)\,,$$
$$T_{cbv}(y, q; f_\nu, f_b, y_d) = y^{-1} D_{cbv}(y, q; f_\nu) T_{\rm master}(q; f_\nu, f_b, y_d)\,, \quad (19)$$

where $T_{\rm master}$ has the small-scale limit of

$$\lim_{q\to\infty} T_{\rm master}(q; f_\nu, f_b, y_d) = \frac{M_d(q)}{14.4q^2}\,, \quad (20)$$

which follows from equations (7) and (17). It is important to note that relation of equation (19) holds independently of the small-scale approximation, namely, that once the growth factors $y^{-1}D_i$ are removed, the transfer functions depend on only a *single* time-independent function of q related to perturbations in the CDM component at the drag epoch. This simplification holds only for $y \gg y_d$; near the drag epoch, the contribution of the decaying mode cannot be neglected. In Eisenstein & Hu (1998b), we exploit the existence of this master function to obtain the full time- and q-dependent transfer functions based on fitting formulae for $T_{\rm master}$.

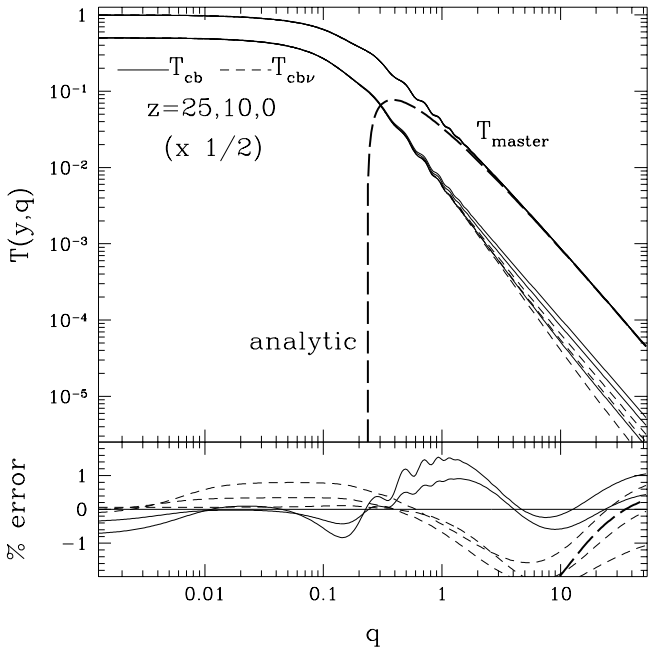

FIG. 3.—Demonstration of the existence of a time-independent master function. The transfer functions for the CDM plus baryon (T_{cb}) and CDM plus baryon plus neutrino (T_{cbv}) fluctuations at three different redshifts are divided by the growth factors D_{cb} and D_{cbv}, respectively, to obtain estimates of $T_{\rm master}$. That the six curves superposed in the upper panel agree at the 1%–2% level (relative to T_{cb}/D_{cb} at $z = 0$, as shown in the lower panel) establishes the existence of the master function and verifies the accuracy of the growth functions. The analytic prediction for $T_{\rm master}$ (*long-dashed line*) converges to within 1% of the numerical results at $q \gg 1$. The model here is $\Omega_0 = 1$, $h = 0.5$, $f_\nu = 0.4$, and $f_b = 0.2$.

We show a comparison between analytic and numerical results in Figure 3. The numerical T_{cb}, T_{cbv} (*lower curves, solid and dashed lines, respectively*) at three different redshifts are plotted here. The upper curve represents the master function $T_{\rm master}$ obtained through inverting the growth factor. Note that six different estimates of $T_{\rm master}$ obtained from T_{cb} and T_{cbv} are superposed and agree at the $\sim$1%–2% level. Also shown is the small-scale prediction of equation (20), which converges rapidly for $q \gtrsim 1$.

Finally, note that the neutrino transfer function is implicitly defined as

$$T_\nu = f_\nu^{-1}(T_{cbv} - f_{cb}\, T_{cb})\,, \quad (21)$$

and its construction from the growth functions and $T_{\rm master}$ yields *density-weighted* errors of the same order as the other transfer functions, i.e., (1%–2%) $\times\, \delta_{cbv}/f_\nu\,\delta_\nu$.

6. LOW-DENSITY MODELS

The formulae presented thus far are valid for $\Omega_0 = 1$ cosmologies. We have, however, shown that the transfer functions today can be expressed as the products of a growth function and a master function related to fluctuations at the drag epoch. At this earlier time, the cosmological constant and curvature have negligible effects on the dynamics. This implies that a simple modification of the growth function at late times to account for $\Omega_0 \neq 1$ effects will suffice for a complete description.

Let us recall that on the largest scales, where neutrino free streaming and radiation pressure gradients are negligible,

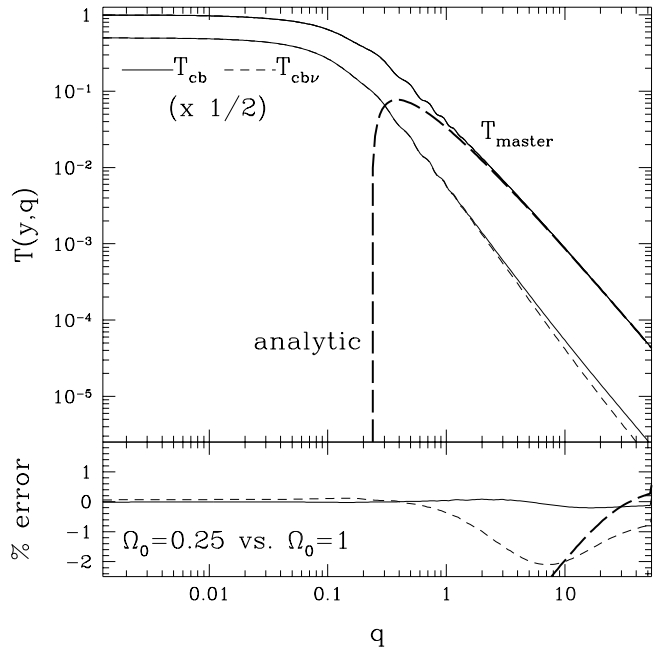

FIG. 4.—Demonstration of the invariance of the master function ($T_{\rm master}$) under changes in the cosmological constant Λ. The model has the same $\Omega_0 h^2, f_b$, and f_ν as Fig. 3 at $z = 0$, but with $\Omega_0 = 0.25$. Division of T_{cb} and $T_{cb\nu}$ by the growth functions returns the master function $T_{\rm master}$ over which the estimate of Fig. 3 and the small-scale analytic solution are plotted (*upper panel*). The errors are plotted relative to $T_{\rm master}$ from the T_{cb}, $z = 0$ estimate of Fig. 3 and show agreement at the 1%–2% level (*lower panel*).

fluctuations grow as (Heath 1977)

$$D(y;\,\Omega_0,\,\Omega_\Lambda) = \frac{5}{2}\,g(y)\int^y \frac{dx}{x^3 g(x)^3}\,, \tag{22}$$

where

$$g^2(y) = y^{-3} + y^{-2}y_0^{-1}(1-\Omega_0-\Omega_\Lambda)/\Omega_0 + y_0^{-3}\,\Omega_\Lambda/\Omega_0\,, \tag{23}$$

with $y_0 = (1 + z_{\rm eq})$. Analytic forms for the $\Omega_\Lambda = 0$ and $\Omega_0 + \Omega_\Lambda = 1$ cases are given in Groth & Peebles (1975) and Bildhauer et al. (1992), respectively. The normalization of the growth rate has been chosen so that $D = y$ at early times. Moreover, equation (22) states that after matter ceases to dominate the expansion rate, fluctuation growth halts.

By matching these asymptotic limits, we can approximate the growth function in the presence of neutrinos by the replacement of y with D, i.e.,

$$D_{cb}(y,\,q;f_\nu,\,\Omega_0,\,\Omega_\Lambda) = \left\{1+\left[\frac{D(y)}{1+y_{\rm fs}(q)}\right]^{0.7}\right\}^{p_{cb}/0.7} D^{1-p_{cb}}(y)\,, \tag{24}$$

$$D_{cb\nu}(y,\,q;f_\nu,\,\Omega_0,\,\Omega_\Lambda) = \left\{f_{cb}^{0.7/p_{cb}}+\left[\frac{D(y)}{1+y_{\rm fs}(q)}\right]^{0.7}\right\}^{p_{cb}/0.7} D^{1-p_{cb}}(y)\,, \tag{25}$$

where, of course, $D(y) = D(y;\,\Omega_0,\,\Omega_\Lambda)$ implicitly. Likewise, the transfer functions become

$$T_{cb}(y,\,q) = D^{-1}(y)D_{cb}(y,\,q)T_{\rm master}(q)\,,$$
$$T_{cb\nu}(y,\,q) = D^{-1}(y)D_{cb\nu}(y,\,q)T_{\rm master}(q)\,. \tag{26}$$

We show an example in Figure 4. The model has been chosen to have $\Omega_0 = 0.25, \Omega_\Lambda = 0.75$ with the same $\Omega_0 h^2, f_b$, and f_ν as Figure 3 and hence the same $T_{\rm master}$. The invariance of the master function is demonstrated by overplotting estimates from T_{cb} and $T_{cb\nu}$ in this model and from T_{cb} of Figure 3. The lower panel shows the fractional difference of the former with respect to the latter.

In principle, the fact that infall freezes out at a later redshift in a Λ versus open cosmology of the same Ω_0 allows one to distinguish between these two alternatives by the shape of the transfer function at a single redshift alone. Massive neutrinos therefore break the *shape degeneracy* of the transfer function in low-density universes. However, since this effect is only significant if $\Omega_0 \ll 1$, the more important fact is that growth in the matter-dominated epoch depends on $(1 - \Omega_\nu/\Omega_0)$; hence, even a relatively small density in neutrinos can make a dramatic effect on the growth rates in a low-density universe. Figure 4 demonstrates that $\Omega_\nu = 0.1$ in an $\Omega_0 = 0.25$ universe gives the same magnitude effects as $\Omega_\nu = 0.4$ in an $\Omega_0 = 1$ universe. Upper limits on Ω_ν from small-scale fluctuations thus tighten for low-density universes (Primack et al. 1995).

7. DISCUSSION

We have presented small-scale solutions to the linear evolution of perturbations in a cold + hot + baryonic dark matter cosmology. They converge to within 1% of the numerical solutions for $q \gg 1$ and $q \gg q_{\rm fs}$ and are expressed in terms of hypergeometric functions in the appendix. We have also given simplified forms in the main text, employing only algebraic functions, which are valid for $\Omega_b + \Omega_\nu \lesssim 0.6\Omega_0$ and $\Omega_0 h^2 \gtrsim 0.1$. Baryons play a significant role in MDM cosmologies since dark matter perturbations are density weighted and depend on $\Omega_b/(\Omega_0 - \Omega_\nu)$ and not on Ω_b/Ω_0. Likewise neutrinos in a low-density universe yield enhanced effects since growth rates depend on Ω_ν/Ω_0.

By comparing analytic and numerical results at $q \lesssim q_{\rm fs}$, we have isolated the effects of neutrino infall and described them to an accuracy of 1%–2% by time- and wavenumber-dependent growth factors for the CDM and total matter. The freeze-out of infall at late times when Λ or curvature come to dominate can similarly be taken into account. We have shown that these growth factors are valid beyond the small-scale approximation.

The full time- and wavenumber-dependent transfer functions for the CDM and total matter can thus be described as a product of these growth factors and a single function of wavenumber related to the amplitude of fluctuations at the Compton drag epoch that in turn depends on $\Omega_0 h^2$, Ω_ν/Ω_0, Ω_b/Ω_0, and the number of degenerate neutrino species. We leave a quantitative description of this master function and implications for constraints on Ω_ν to a companion paper (Eisenstein & Hu 1998b).

W. H. and D. J. E. are supported by NSF PHY 95-13835. W. H. was additionally supported by the W. M. Keck Foundation. Numerical results were extracted from the CMB fast package of Seljak & Zaldarriaga (1996), version 2.3.

APPENDIX

DERIVATION OF THE SMALL-SCALE SOLUTION

Following the analytic approach of HS96, one can solve the equation of motion for the CDM on small scales where the gravitational effects of the MDM can be neglected. The idea is to separate the evolution before and after the drag epoch. Before the drag epoch, the gravitational effects of the baryons can be ignored below the sound horizon as they are pressure supported by the photons. The equation of motion then becomes

$$\ddot{\delta}_c + \frac{\dot{a}}{a}\dot{\delta}_c = \frac{3}{2a} f_c \Omega_0 H_0^2 \delta_c \,, \tag{A1}$$

where overdots indicate derivatives with respect to conformal time η. Unfortunately, the complicated equation of state of massive neutrinos prevents the time evolution of the scale factor $a(\eta)$ from being written down in closed form. However, we know that the neutrinos behave as radiation at early times when $T_\nu \gg m_\nu$ and as matter at late times when $T_\nu \ll m_\nu$. These limits are identical to those found if one considered the neutrinos to be massless and added their mass to that of the nonrelativistic matter. It is therefore a reasonable first approximation to leave the background evolution unmodified by the replacement of a portion of the nonrelativistic matter with massive neutrinos, i.e.,

$$\eta = 2(\Omega_0 H_0^2)^{-1/2}(1 + z_{\rm eq})^{-1/2}(\sqrt{1+y} - 1) \,, \tag{A2}$$

where $y = (1 + z_{\rm eq})/(1 + z)$. Here, $z_{\rm eq}$ (eq. [1]) assumes three *massless* neutrino species with the usual thermal history. We neglect cosmological constant and curvature effects here (see § 6). This form otherwise errs only between $z_{\rm eq}$ and the epoch at which the neutrinos become nonrelativistic. Our approach will be to use this approximation to solve the small-scale limit analytically and then correct for a $\lesssim 5\%$ modification due to changes in the expansion rate.

With this approximation, equation (A1) can be rewritten in terms of $y \equiv (1 + z_{\rm eq})/(1 + z)$ as

$$\frac{d^2}{dy^2}\delta_c + \frac{(2+3y)}{2y(1+y)}\frac{d}{dy}\delta_c = \frac{3}{2y(1+y)} f_c \delta_c \,. \tag{A3}$$

As shown in HS96, the general solution to this equation is given through Gauss's hypergeometric function F (also written ${}_2F_1$):

$$U_i = (1+y)^{-\alpha_i} F\left(\alpha_i, \alpha_i + \frac{1}{2}, 2\alpha_i + \frac{1}{2}; \frac{1}{1+y}\right) , \tag{A4}$$

where $i = 1, 2$, and

$$\alpha_i = \frac{1 \mp \sqrt{1 + 24 f_c}}{4} \,, \tag{A5}$$

with minus and plus for $i = 1$ and $i = 2$, respectively. It is useful to note that $\lim_{y\to\infty} U_i = y^{-\alpha_i}$; thus, the two solutions represent the growing and decaying mode for $i = 1$ and 2, respectively. Clearly, $\alpha_1 + \alpha_2 = \frac{1}{2}$.

We obtain the amplitude of the growing and decaying mode by matching onto the $y \ll 1$ solution of HS96 equation (B12),[4]

$$\delta_c = 9.50 \ln(9.24 q y)\Phi(0, q) \,, \qquad y \ll 1 \,, \tag{A6}$$

to find

$$\delta_c(y, q) = 9.50[A_1(q)U_1(y) + A_2(q)U_2(y)]\Phi(0, q) \,, \qquad y < y_d \,, \tag{A7}$$

where the matching coefficients are

$$A_1(q) = \frac{\Gamma(\alpha_1)\Gamma(\alpha_1 + 1/2)}{\Gamma(2\alpha_1 + 1/2) 2\pi \cot(2\pi\alpha_1)} [\ln(9.04q) + 2\psi(1) - 2\psi(1 - 2\alpha_1) - 2\ln 2] \,, \tag{A8}$$

with $\psi(x) = \Gamma'(x)/\Gamma(x)$. The expression for A_2 follows from equation (A8) with the replacement $1 \to 2$ in the subscripts.

Equation (A7) takes the evolution up to the drag epoch. After the drag epoch, the baryons are released from the photons and behave as CDM. The equation of motion for the combined CDM plus baryon system is the same as equation (A3) but with the replacements

$$\delta_c \to \frac{f_c}{f_{cb}}\delta_c + \frac{f_b}{f_{cb}}\delta_b \equiv \delta_{cb} \,, \qquad f_c \to f_{cb} \,, \tag{A9}$$

[4] The numerical factors here reflect the kick a perturbation gets at horizon crossing deep in the radiation-dominated epoch. They are calibrated to agree at the 1% level with CMBfast version 2.3 (high-precision version) and represent a 1%–2% shift vs. the calibration of HS96 based on Sugiyama (1995). Our calibration also matches the code of M. White (Hu et al. 1995) at the 1% level.

and therefore has the same solutions as given by equation (A4) with arguments

$$\tilde{\alpha}_i = \frac{1 \pm \sqrt{1 + 24 f_{cb}}}{4} . \tag{A10}$$

The full solution for δ_{cb} is now found by matching the solution of equation (A7) onto the new growing and decaying modes. Since the decaying mode becomes unimportant for $y \gg y_d$,

$$\delta_{cb}(y, q) = 9.50 M_d(q) \tilde{U}_1(y) \Phi(0, q) , \tag{A11}$$

where

$$M_d(q) = \frac{f_c}{f_{cb}} \left[\frac{\tilde{U}'_2(A_1 U_1 + A_2 U_2) - \tilde{U}_2(A_1 U'_1 + A_2 U'_2)}{\tilde{U}_1 \tilde{U}'_2 - \tilde{U}'_1 \tilde{U}_2} \right] \Bigg|_{y = y_d} \tag{A12}$$

gives the matching condition.

Furthermore, the baryons fall into CDM potential wells at the drag epoch and subsequently follow them so that

$$\delta_{cb} = \delta_c = \delta_b , \qquad y \gg y_d . \tag{A13}$$

For high $\Omega_0 h^2 \gtrsim 0.1$ (or $h \gtrsim 0.3$), $y_d \gg 1$ so that the decaying-mode contribution to equation (A11) coming through U_2 is negligible. Furthermore, the growing mode can be expanded in powers of $(1 + y_d)^{-1}$ as

$$M_d(q) \approx \frac{f_c}{f_{cb}} \frac{2(\tilde{\alpha}_1 + \alpha_1) - 1}{4\tilde{\alpha}_1 - 1} (1 + y_d)^{\tilde{\alpha}_1 - \alpha_1} \left\{ 1 + (1 + y_d)^{-1} \frac{\alpha_1 - \tilde{\alpha}_1}{2} \left[1 + \frac{1}{(4\alpha_1 + 1)(4\tilde{\alpha}_1 - 3)} \right] \right\} A_1(q) . \tag{A14}$$

The approximation holds for $f_c \gtrsim 0.2$. Note that the apparent divergence at $f_c = 0.125$ or $\alpha_1 = -\frac{1}{4}$ disappears once the decaying mode is properly included.

The quantity A_1 can either be evaluated from equation (A8) or approximated as

$$A_1(q) = (1 - 0.553 f_{vb} + 0.126 f_{vb}^3) \ln (1.84 \beta_c q) , \tag{A15}$$

with

$$\beta_c \equiv \exp [-2\psi(2\alpha_2) - 2\psi(3)] \approx (1 - 0.949 f_{vb})^{-1} , \tag{A16}$$

which is valid at the 1% level for $f_{vb} \lesssim \frac{2}{3}$. Finally, we correct for the change in the background expansion rate by comparing equation (A11) to an numerical integration of equation (A1) and find the small correction

$$A_1(q) \rightarrow \frac{A_1(q)}{1 - 0.193 \sqrt{f_\nu N_\nu} + 0.169 f_\nu N_\nu^{0.2}} , \tag{A17}$$

for $f_\nu \lesssim 0.6$. With the identities $\alpha_1 = p_c - 1$ and $\tilde{\alpha}_1 = p_{cb} - 1$, the derivation of the small-scale evolution (eq. [4]) is now complete.

REFERENCES

Bildhauer, S., Buchert, T., & Kasai, M. 1992, A&A, 263, 23
Bond, J. R., Efstathiou, G., & Silk, J. 1980, Phys. Rev. Lett., 45, 1980
Bond, J. R., & Szalay, A. S. 1983, ApJ, 274, 443
Dodelson, S., Gates, E., & Stebbins, A. 1996, ApJ, 467, 10
Eisenstein, D. J., & Hu, W. 1998a, ApJ, 496, in press
———. 1998b, ApJ, submitted
Fixsen, D., et al. 1996, ApJ, 473, 576
Groth, E. J., & Peebles, P. J. E. 1975, A&A, 41, 143
Heath, D. J. 1977, MNRAS, 179, 351
Hu, W., Scott, D., Sugiyama, N., & White, M. 1995, Phys. Rev. D, 52, 5498
Hu, W., & Sugiyama, N. 1996, ApJ, 471, 542 (HS96)
Kauffmann, G., & Charlot, S. 1994, ApJ, 430, L97
Klypin, A., Borgani, S., Holtzman, J. A., & Primack, J. R. 1995, ApJ, 441, 1
Ma, C.-P. 1996, ApJ, 471, 13
Ma, C.-P., & Bertschinger, E. 1995, ApJ, 455, 7
Ma, C.-P., Bertschinger, E., Hernquist, L., Weinberg, D. H., & Katz, N. 1997, ApJ, 484, L1
Mo, H. J., & Fukugita, M. 1996, ApJ, L9
Mo, H. J., & Miralda-Escudé, J. 1994, ApJ, 430, L25
Primack, J. R., Holtzman, J., Klypin, A., Caldwell, D. A. 1995, Phys. Rev. Lett., 74, 2160
Rugers, M., & Hogan, C. J. 1996, ApJ, 459, L1
Seljak, U., & Zaldarriaga, M. 1996, ApJ, 469, 437
Steidel, C. C., Giavalisco, M., Pettini, M. Dickinson, M., & Adelberger, K. L. 1996, ApJ, 462, L17
Sugiyama, N. 1995, ApJS, 100, 281
Tytler, D., Fan, X. M., & Burles, S. 1996, Nature, 381, 207
Walker, T. P., Steigman, G., Kang, H., Schramm, D. M., & Olive, K. A. 1991, ApJ, 376, 51
Weinberg, D. H., Miralda-Escudé, J., Hernquist, L., & Katz, N. 1997, ApJ, 490, 564